SF2A 2012
S. Boissier, P. de Laverny, N. Nardetto, R. Samadi, D. Valls-Gabaud and H. Wozniak (eds)

LENSING IN CLUSTERS

R. Cabanac[1]

Abstract. This review is based on the paper of Kneib & Natarajan (2011). I briefly review the strong lensing methods and presents the main results Strong Lensing studies achieved in recent years in the domain of clusters of galaxies.

Keywords: Gravitational lensing: strong, Galaxies:clusters:general

1 Introduction

In recent years, the release of large and deep imaging and spectroscopic surveys has increased the use of large samples of strong lensing candidates to study the dark components of the universe. In turn, this has triggered the community to improve modelling tools and better understand systematics, which are a chief concern of strong lensing cosmological studies. Section one outlines the methods used in lensing, Section two presents studies on mass distribution in clusters, Section three and four compares observed properties with theoretical predictions, and Section five introduces the coming ground-based and space borne instruments.

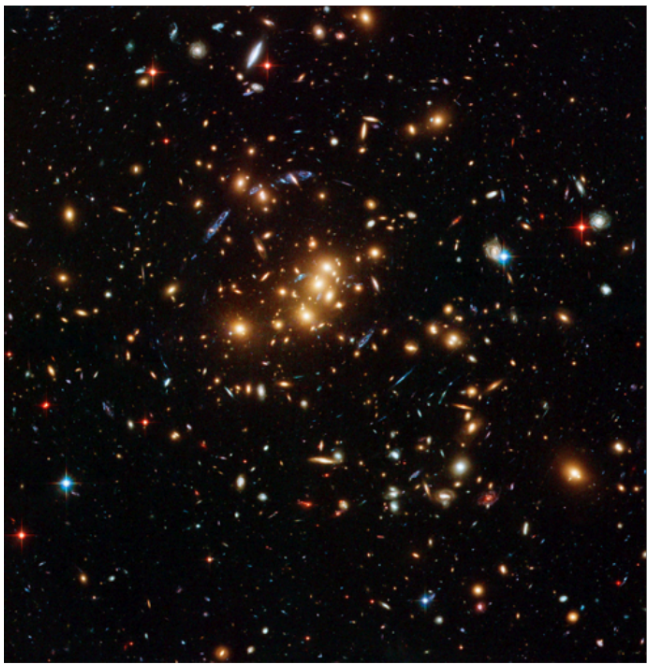

Fig. 1. Strong Lensing arcs in cluster Cl0024+1654 at redshift z=0.395 (HST ACS imaging)

[1] OMP, 57 Ave d'Azereix, 65000, Tarbes, France

2 Contraining cluster mass distributions with lensing

The General Relativity theory provides an elegant interpretation of large arcs witnessed in deep imaging of some clusters, the theory has been described in Schneider, Ehlers & Falco (Schneider et al. 1992), interested readers are refered to their monography. In summary, Lensing effects are space-time deformations induced by massive over-densities

We will focus on the application to massive clusters at redshifts $z \sim 0.2$-0.5, which are well approximated as single-plane lenses. Lensing effect actually probes the 2-D Newton potential $\phi(x, y)$ from a 3-D density distribution $\rho(x, y, z)$. The projected surface mass density is $\Sigma(x, y) = \frac{\nabla^2\phi(x,y)}{4\pi G}$.

Lensing effect maps a source plane into a image plane and is usually parametrized in terms three vectors: convergence κ, shear γ and deflection angles $\overrightarrow{\alpha}$

$\overrightarrow{\alpha}(\overrightarrow{\theta}) = \overrightarrow{\nabla}_{\overrightarrow{\theta}}\varphi(\overrightarrow{\theta})$, $\kappa(\overrightarrow{\theta}) = \frac{1}{2}\left(\frac{\partial^2\varphi}{\partial\theta_1^2} + \frac{\partial^2\varphi}{\partial\theta_2^2}\right)$, $\gamma^2(\overrightarrow{\theta}) = \| \gamma(\overrightarrow{\theta}) \|^2 = \frac{1}{4}\left(\frac{\partial^2\varphi}{\partial\theta_1^2} - \frac{\partial^2\varphi}{\partial\theta_2^2}\right)^2 + \left(\frac{\partial^2\varphi}{\partial\theta_1\partial\theta_2}\right)$.

2.1 Strong lensing modeling

Modeling approaches : Two methods of modelling are used in the community. Parametric modelling is physically motivated and uses small number of clumps to describe the mass density potential (Kneib et al. 1996; Natarajan & Kneib 1996). Non-parametric methods use tesselated (pixelized) mass distributions with no prior (Saha & Williams 1997; Diego et al. 2005; Coe et al. 2010). The two methods are complementary and usually converge towards similar results.

From simple to more complex : The fundamental parameter that lensing events tell the observer is the total mass contained within the Einstein radius, given by: $M(< \theta_E) = \pi\Sigma_{crit}D_{OL}^2\theta_E^2$, where θ_E is the location of the tangential critical line for a circular mass distribution, usually approximated by the tangential arc radius, Σ_{crit} is the critical density, D_{OL} is the angular distance between the observer and the lens.
For non-circular distributions and profiles additional constraints are used, for instance, arcs at different radii are very useful to probe the shape of dark matter profiles. In particular, radial arcs are unique probe to the center surface density (Fort et al. 1992; Smith et al. 2001; Sand et al. 2005; Gavazzi et al. 2003)
The proper way (commonly used in the community) to accurately constrain the mass in cluster cores is thus to use multiple-images with preferably measured spectroscopic redshifts to absolutely calibrate the mass. To do this, one generally denes a likelihood $\pounds$ for the observed data D and parameters p of the model, N systems, n_i images: $\pounds = Pr(D|p) = \prod_{i=1}^{N} \frac{1}{\prod_{j=1}^{n_i}\sigma_{ij}\sqrt{2\pi}} exp^{-\chi^2/2}$ and each image contributes to $\chi_i^2 = \sum_{j=1}^{n_i}\frac{(\theta_{obj}^j - \theta_p^j)^2}{\sigma_{ij}^2}$. θ_p^j is the position predited by model p, and σ_{ij}^2 are errors. For extended arc images, non-parametric pixellated modelling is the only way to take into account the S/N of each image (Dye & Warren 2005; Suyu et al. 2006), but rather combersome for clusters because many images are often involved over large areas. Finally, selecting lensed images is an iterative process, which must be done by humans, a physically motivated mass speed up the process.

Parametric modeling of the various cluster mass components : A good cluster lens model must have Dark Halo(s) for the cluster component(s) ϕ_{c_i} (DM + intracluster gas), Dark halos around massive galaxies (truncated because of tidal stripping) ϕ_{p_j}, the total potentiel being the sum of all components, $\phi_{tot} = \sum_i \phi_{c_i} + \sum_i \phi_{p_j}$. A popular model for galaxies is the physically motivated PIEMD (Brainerd et al. 1996), that allows probing trucation and various mass/light ratio (Limousin et al. 2008; Leauthaud et al. 2011, in COSMOS).

Bayesian modeling : State-of-the-art parametric modelling (LENSTOOL, `http://www.oamp.fr/cosmology/lenstool/`, (Jullo et al. 2007)) is performed using Bayesian inference. The Bayesian approach allows a better parameter exploration and model comparison under the intrinsic degeneracies of lens modeling.

$Pr(p|D, M) = \frac{Pr(D|p,M)Pr(p|M)}{Pr(D|M)}$

Probing the radial profile of the mass in cluster cores : As already mentionned strong lensing arcs are the only observable able to probe the inner profile of DM at the center of clusters. It is important because DM only simulations predict cluster core shapes $\rho_{DM} \propto r^{-\beta}$ and $\beta = -1$ NFW or $\beta = -1.5$ (Moore et al. 1998). Most precise techniques combine stellar dynamics in triaxial halo with lensing to compute independent profiles for DM and Baryonic matter. All recent results on Abell 383 point towards a DM $\beta < -1$. A lot of work is ongoing

for other clusters.

Recent non-parametric strong lensing modeling: With advent of very high-quality data set. Non-parametric modelling is becoming popular (Coe et al. 2010; Zitrin et al. 2010). Non-parametric models replace profiles by pixel (or radial basis function) maps. Due to a large number of degrees of freedom, non-parametric models lead to more flexibility to probe a wide range of mass distributions (Bradač et al. 2005, Bullet cluster). A drawback is that non-parametric model are difficult to interpret and do not take into account known components (e.g. galaxy scale clumps). Hybrid schemes partially solving this problem (mixing parametric and non-parametric techniques are promising (Jullo & Kneib 2009).

2.2 Cluster weak lensing modeling

At larger radii from cluster centers, in subcritical areas, the only available lensing signal is weak lensing. Weak lensing signal in outskirks of clusters must be treated statistically ($\sim$ percent level) and is prone to strong observational errors (PSF variations, foreground contamination). Reconstruction methods are not straitghtforward, but the large number of lensed objects make it useful. A lot of observations are now available either from space with Hubble Space Telescope, and ground with CFHT12K (Bardeau et al. 2007; Hoekstra 2007), Megacam (Gavazzi & Soucail 2007) (Shan et al. 2010), SuprimeCam (Okabe et al. 2010). A lot of progress has also been done on the measurements of galaxy shapes: using a clean sample, the direct method is IMCAT (Kaiser et al. 1995), (Rhodes et al. 2000; Hoekstra 2000), reverse method IM2SHAPE (Bridle et al. 2002), LENSFIT (Kitching et al. 2008) and SHAPELETS (Refregier & Bacon 2003). The best methods have improved through challenges STEP, GREAT8 and 10 (Bridle et al. 2010; Kitching et al. 2012).
Measuring total mass and mass profiles: Direct methods to extract weak lensing signals are aperture mass densitometry (Fahlman et al. 1994). Clowe (1998) proposes to sum up tangential weak shear within a radius θ_1. $M(<\theta) = \pi D_{OL}^2 \theta^2 \Sigma_{crit} \zeta(\theta)$ (Hetterscheidt et al. 2005; Hoekstra 2007; Okabe et al. 2010, e.g.), that method assumes that all background galaxies are at same redshift. Semi-direct methods use surface density estimator (Mandelbaum et al. 2005) : $\Delta\Sigma(r)$, this estimator is then computed directly from parametrized models (Gruen et al. 2011).Finally, one can use a parametric method by fitting directly the weak lensing signal with a parametric model (following strong lensing methods). (Metzler et al. 1999, 2001; King et al. 2001).
Cluster triaxiality: Spherical symetry is not a good approximation for clusters. Triaxial cluster can explain observed discrepancy between the high concentration measured in lensing clusters with regard to DM simulations. (Gavazzi 2005). This is the case fro A1689 (Andersson & Madejski 2004; Lemze et al. 2008; Peng et al. 2009). Combining X-rays, Sunyaev-Zeldovich (SZ) and lensing analyses allows us to probe triaxiality (Mahdavi et al. 2007, on A478). Morandi et al. (2010) Study on MACS J1423.8+2404 shows a triaxial halo with axial ratio 1.53±0.15 (plane of sky) and 1.44±0.07 (line of sight).

3 Mass distribution of cluster samples

Compare lensing analysis of cluster samples with X-ray luminosity, temperature, velocity dispersions, SZ effect. Are cluster relaxed? How much substructure in clusters? How triaxial are they? What are the signatures of merger events? How important are projections? Observations can be compared to numerical simulations in order to test formation paradigm. The challenge is to define and collect a statistically significant dataset spanning a range of spatial scales. Early work: Luppino et al. (1999); Dahle et al. (2002); Smith et al. (2003). Lensing clusters imaged by HST are likely to be biased toward massive end at all redshifts. (+ projection effects). X-ray selection is less biased $\propto$ ICM electron density^2, Smith et al. (2005) finds in 12 clusters $z \sim 0.2$ $L_X > 8 \times 10^{44}$erg/s (0.1-2.4 keV) from XBACS catalog. 70% of that sample shows strong lensing signal. Smith et al. define dynamical relaxation as: a dominant core ($M_{core}/M_{tot} > 0.95$), a dominant central galaxy, and alignment between x-ray and mass distrib. 7 clusters are disturbed, bi or tri modal implying recent merging activities. In contrast, Bardeau et al. (2007) did not see such a difference using CFHT12K imaging. New samples are very much needed but hard to build, work using 50 X-ray clusters is ongoing Hoekstra et al. (2012, Canadian Cluster Comparison Project).

3.1 On-going and future cluster lensing surveys

4 techniques are used to search for clusters; (i) photometric searches : Red-sequence surveys (Gladders 2002), CFHTLS, new surveys starting VST KIDS, Dark Energy Survey (DES). (ii) X-ray selected cluster: ROSAT

based MAssice Cluster Survey (MACS Ebeling et al. 2001; Böhringer et al. 2004, REFLEX) dedicated search WARPS, SHARC, ROSAT deep cluster survey, XMM DCS, XMM LSS (Scharf et al. 2005; Rosati et al. 2002). (iii) SZ search: Atacama Cosmology Telescope Cluster survey (Marriage et al. 2011). South Pole Telescope Cluster survey (Plagge et al. 2010), and Planck. (iv) Weak and strong lensing searched based on photometric surveys or follow-up of x-ray and SZ clusters.

3.2 Targeted cluster surveys

The Local Cluster Substructure Survey (LoCuSS): extend Smith et al. (2005) goals: get mass, structure and thermodynamics of a volume of ~ 80 clusters $0.15 < z < 0.3$ limited sample (Richard et al. 2010), weak lensing of 30 clusters. Principal results: NFW profiles confirmed, Mass concentration relation consistent with ΛCDM (contrary to previous work on large Einstein radius clusters!). First SZ-WL results on 18 clusters, seems to confirm a projection bias for WL prolate undisturbed clusters compared to disturbed clusters (Okabe et al. 2010; Zhang et al. 2010; Marrone et al. 2012).
The MAssive Cluster Survey: 124 X-ray luminous clusters $0.3 < z < 0.7$: many are strong lenses (Zitrin et al. 2011, 12 clusters HST follow-up $z > 0.5$). Many clusters being studied (Limousin et al. 2010, 2012; Morandi et al. 2010). MACSJ0717.5+3745 shows a merger of four structures (Jauzac et al. 2012) weak lensing measurement using 18 pointings HST). MACS sample is significantly richer in arcs than RCS.
ESO distant cluster survey: $z > 0.6$ optical selection of 20 fields of Las Campanas Distant Cluster Survey. Spectroscopy and photomery follow-ups on the most distants clusters. Clowe et al. (2006b) compare mass measurements of 13 EDiSC clusters with luminosities and finds dependence of cluster mass-to-light ratio with redshift.
Red-sequence cluster survey (Gladders 2002). RCS2 1000 deg^2, among 10^4 cluster sample, a small sub-sample show strong lensing events. Appart from identifying them nothing was done yet on them.
The Multi-Cluster Treasury: ongoing CLASH survey, Postman et al. HST follow-up of 20 X-ray clusters.

3.3 Cluster lenses in wide cosmological surveys

Non targeted surveys are rich source of lenses at all scales. They triggered new automated detection procedures and are much need to prepare massive data from EUCLID. The SDSS, although not optimized for lens search (too shallow, poor seeing). Henawi et al. discovers 16 lenses, 21 candidates among 240 clusters. Those samples are statistically clean, will help defining selection functions. Kubo et al. (2009) identify 10 strong lenses in the Sloan Bright Arc Survey. Bayliss et al. (2011); Bayliss (2012) follow-up 26 Strong lensing cluster among SDSS/RCS. The CFHTLS: SL2S (Cabanac et al. 2007; More et al. 2012), 40 group scale, 120 candidates. Limousin et al. (2009) studied mass and light distribution of 13 groups, encovering redshift trends in mass and groups luminosities. Group lensing is a niche for flexion analysis. First large-scale structure maps of lenses. CFHTLS: weak lensing on Deep fields (Gavazzi & Soucail 2007). First maps of weak lensing peaks. Catalog of lensing selected clusters (Shan et al. 2012). Bergé et al. (2008) combined analysis of XMM-LSS and CFHTLS , contrained $\sigma_8 = 0.92^{+0.26}_{-0.30}$. COSMOS: very deep, allows probing fainter clusters at higher redshift. Faure et al. (2008, 2009, 2011), Strong Lensing map of COSMOS $z < 2$ no correlation between lens loci and COSMOS large structures. Leauthaud et al. (2010): weak lensing study of 200 x-ray groups.

4 Comparison of observed lensing cluster properties with theoretical predictions

Internal structure of cluster halos Cosmological DM-only simulations predict NFW profiles for clusters over a large range of range of scales.
On the observational side, lensing analyses probe total mass in the inner 0.1-5 Mpc and tend to show various inner concentrations. Plausible errors in lensing explaining such difference between predictions and observations are contaminations of other structure line of sight, projection biases, and physical feedback of baryons over DM (Comerford & Natarajan 2007).
Mass function of substructure in cluster halos No substructure crisis in clusters between ΛCDM (Springel et al. 2005, Millenium) and galaxy-galaxy lensing analyses in clusters. (Natarajan et al. 2007). Substructure crisis at galaxy scales must come from evolutionary reasons (e.g. baryonic feedback). Group-scale analyses shall also be interesting!

Does Dark Matter exist? The bullet cluster and other clusters showing different distributions between WL and ICM are convincing (Bradač et al. 2006; Clowe et al. 2006a).

5 Future prospects

Space missions: JWST, EUCLID, WFIRST(?) and ground-based project (LSST, DES, TMT?, E-ELT) will bring lensing studies into a distinct new level.
Radio observations: ALMA (SKA?) is expected to boost the field of lensed galaxy combining velocity field data and galaxy shapes.

References

Andersson, K. E. & Madejski, G. M. 2004, ApJ, 607, 190
Bardeau, S., Soucail, G., Kneib, J.-P., et al. 2007, A&A, 470, 449
Bayliss, M. B. 2012, ApJ, 744, 156
Bayliss, M. B., Gladders, M. D., Oguri, M., et al. 2011, ApJ, 727, L26
Bergé, J., Pacaud, F., Réfrégier, A., et al. 2008, MNRAS, 385, 695
Böhringer, H., Schuecker, P., Guzzo, L., et al. 2004, A&A, 425, 367
Bradač, M., Clowe, D., Gonzalez, A. H., et al. 2006, ApJ, 652, 937
Bradač, M., Erben, T., Schneider, P., et al. 2005, A&A, 437, 49
Brainerd, T. G., Blandford, R. D., & Smail, I. 1996, ApJ, 466, 623
Bridle, S., Balan, S. T., Bethge, M., et al. 2010, MNRAS, 405, 2044
Bridle, S. L., Kneib, J.-P., Bardeau, S., & Gull, S. F. 2002, in The Shapes of Galaxies and their Dark Halos, ed. P. Natarajan, 38–46
Cabanac, R. A., Alard, C., Dantel-Fort, M., et al. 2007, A&A, 461, 813
Clowe, D., Bradač, M., Gonzalez, A. H., et al. 2006a, ApJ, 648, L109
Clowe, D., Schneider, P., Aragón-Salamanca, A., et al. 2006b, A&A, 451, 395
Clowe, D. I. 1998, PhD thesis, UNIVERSITY OF HAWAII
Coe, D., Benítez, N., Broadhurst, T., & Moustakas, L. A. 2010, ApJ, 723, 1678
Comerford, J. M. & Natarajan, P. 2007, MNRAS, 379, 190
Dahle, H., Kaiser, N., Irgens, R. J., Lilje, P. B., & Maddox, S. J. 2002, ApJS, 139, 313
Diego, J. M., Protopapas, P., Sandvik, H. B., & Tegmark, M. 2005, MNRAS, 360, 477
Dye, S. & Warren, S. J. 2005, ApJ, 623, 31
Ebeling, H., Edge, A. C., & Henry, J. P. 2001, ApJ, 553, 668
Fahlman, G., Kaiser, N., Squires, G., & Woods, D. 1994, ApJ, 437, 56
Faure, C., Anguita, T., Alloin, D., et al. 2011, A&A, 529, A72
Faure, C., Kneib, J.-P., Covone, G., et al. 2008, ApJS, 176, 19
Faure, C., Kneib, J.-P., Hilbert, S., et al. 2009, ApJ, 695, 1233
Fort, B., Le Fevre, O., Hammer, F., & Cailloux, M. 1992, ApJ, 399, L125
Gavazzi, R. 2005, A&A, 443, 793
Gavazzi, R., Fort, B., Mellier, Y., Pelló, R., & Dantel-Fort, M. 2003, A&A, 403, 11
Gavazzi, R. & Soucail, G. 2007, A&A, 462, 459
Gladders, M. D. 2002, PhD thesis, Department of Astronomy and Astrophysics, University of Toronto
Gruen, D., Bernstein, G. M., Lam, T. Y., & Seitz, S. 2011, MNRAS, 416, 1392
Hetterscheidt, M., Erben, T., Schneider, P., et al. 2005, A&A, 442, 43
Hoekstra, H. 2000, PhD thesis, Kapteyn Astronomical Institute, Groningen, The Netherlands
Hoekstra, H. 2007, MNRAS, 379, 317
Hoekstra, H., Mahdavi, A., Babul, A., & Bildfell, C. 2012, ArXiv e-prints (1208.0606)
Jauzac, M., Jullo, E., Kneib, J.-P., et al. 2012, ArXiv e-prints (1208.4323)
Jullo, E. & Kneib, J.-P. 2009, MNRAS, 395, 1319
Jullo, E., Kneib, J.-P., Limousin, M., et al. 2007, New Journal of Physics, 9, 447
Kaiser, N., Squires, G., & Broadhurst, T. 1995, ApJ, 449, 460

King, L. J., Schneider, P., & Springel, V. 2001, A&A, 378, 748
Kitching, T. D., Balan, S. T., Bridle, S., et al. 2012, MNRAS, 423, 3163
Kitching, T. D., Miller, L., Heymans, C. E., van Waerbeke, L., & Heavens, A. F. 2008, MNRAS, 390, 149
Kneib, J.-P., Ellis, R. S., Smail, I., Couch, W. J., & Sharples, R. M. 1996, ApJ, 471, 643
Kubo, J. M., Allam, S. S., Annis, J., et al. 2009, ApJ, 696, L61
Leauthaud, A., Finoguenov, A., Kneib, J.-P., et al. 2010, ApJ, 709, 97
Leauthaud, A., Tinker, J., Behroozi, P. S., Busha, M. T., & Wechsler, R. H. 2011, ApJ, 738, 45
Lemze, D., Barkana, R., Broadhurst, T. J., & Rephaeli, Y. 2008, MNRAS, 386, 1092
Limousin, M., Cabanac, R., Gavazzi, R., et al. 2009, A&A, 502, 445
Limousin, M., Ebeling, H., Ma, C.-J., et al. 2010, MNRAS, 405, 777
Limousin, M., Ebeling, H., Richard, J., et al. 2012, A&A, 544, A71
Limousin, M., Richard, J., Kneib, J.-P., et al. 2008, A&A, 489, 23
Luppino, G. A., Gioia, I. M., Hammer, F., Le Fèvre, O., & Annis, J. A. 1999, A&AS, 136, 117
Mahdavi, A., Hoekstra, H., Babul, A., et al. 2007, ApJ, 664, 162
Mandelbaum, R., Hirata, C. M., Seljak, U., et al. 2005, MNRAS, 361, 1287
Marriage, T. A., Acquaviva, V., Ade, P. A. R., et al. 2011, ApJ, 737, 61
Marrone, D. P., Smith, G. P., Okabe, N., et al. 2012, ApJ, 754, 119
Metzler, C. A., White, M., & Loken, C. 2001, ApJ, 547, 560
Metzler, C. A., White, M., Norman, M., & Loken, C. 1999, ApJ, 520, L9
Moore, B., Governato, F., Quinn, T., Stadel, J., & Lake, G. 1998, ApJ, 499, L5
Morandi, A., Pedersen, K., & Limousin, M. 2010, ApJ, 713, 491
More, A., Cabanac, R., More, S., et al. 2012, ApJ, 749, 38
Natarajan, P., De Lucia, G., & Springel, V. 2007, MNRAS, 376, 180
Natarajan, P. & Kneib, J.-P. 1996, MNRAS, 283, 1031
Okabe, N., Takada, M., Umetsu, K., Futamase, T., & Smith, G. P. 2010, PASJ, 62, 811
Peng, E.-H., Andersson, K., Bautz, M. W., & Garmire, G. P. 2009, ApJ, 701, 1283
Plagge, T., Benson, B. A., Ade, P. A. R., et al. 2010, ApJ, 716, 1118
Refregier, A. & Bacon, D. 2003, MNRAS, 338, 48
Rhodes, J., Refregier, A., & Groth, E. J. 2000, ApJ, 536, 79
Richard, J., Smith, G. P., Kneib, J.-P., et al. 2010, MNRAS, 404, 325
Rosati, P., Borgani, S., & Norman, C. 2002, ARA&A, 40, 539
Saha, P. & Williams, L. L. R. 1997, MNRAS, 292, 148
Sand, D. J., Treu, T., Ellis, R. S., & Smith, G. P. 2005, ApJ, 627, 32
Scharf, C. A., Zurek, D. R., & Bureau, M. 2005, ApJ, 633, 154
Schneider, P., Ehlers, J., & Falco, E. E. 1992, Gravitational Lenses (Berlin: Springer-Verlag)
Shan, H., Kneib, J.-P., Tao, C., et al. 2012, ApJ, 748, 56
Shan, H. Y., Qin, B., & Zhao, H. S. 2010, MNRAS, 408, 1277
Smith, G. P., Edge, A. C., Eke, V. R., et al. 2003, ApJ, 590, L79
Smith, G. P., Kneib, J.-P., Ebeling, H., Czoske, O., & Smail, I. 2001, ApJ, 552, 493
Smith, G. P., Kneib, J.-P., Smail, I., et al. 2005, MNRAS, 359, 417
Springel, V., White, S. D. M., Jenkins, A., et al. 2005, Nature, 435, 629
Suyu, S. H., Marshall, P. J., Hobson, M. P., & Blandford, R. D. 2006, MNRAS, 371, 983
Zhang, Y.-Y., Okabe, N., Finoguenov, A., et al. 2010, ApJ, 711, 1033
Zitrin, A., Broadhurst, T., Barkana, R., Rephaeli, Y., & Benítez, N. 2011, MNRAS, 410, 1939
Zitrin, A., Broadhurst, T., Umetsu, K., et al. 2010, MNRAS, 408, 1916